Patterns on a surface: the reconciliation of the circle and the square

Chris J K Williams
Department of Architecture & Civil Engineering
University of Bath
Bath BA2 7AY
UK

Abstract

The theory of heat flow on a surface shows that any curvilinear quadrilateral can be 'tiled' with curvilinear squares of varying size. This paper demonstrates a simple numerical technique for doing this that can also be applied to shapes other than quadrilaterals. In particular, any curvilinear triangle can be tiled with curvilinear equilateral triangles.

Keywords

Differential geometry, tiling, tension coefficient, harmonic coordinates, isothermal coordinates, dynamic relaxation.

Introduction

This paper arose out of a re-examination of the way in which the geometry of the British Museum Great Court roof (figure 1) was derived by defining a single surface in the form $z = f(x,y)$ and then relaxing a grid over the surface [1]. Figure 2 shows the structural grid in black and a finer grid in blue that was used for the relaxation process. There was no particular requirement that the triangles of the structural grid should be equilateral, other structural and architectural issues were more pressing. Nevertheless it is an interesting question as to whether all the triangles could have been made equilateral.

In the theoretical discussion in this paper we shall assume that we are dealing with a 'fine' grid so that there is little difference between behaviour of the grid and the equivalent continuum as described by classical differential geometry. The Geometric Modelling and Industrial Geometry Research Unit at TU Vienna makes a special study of the discrete differential geometry of coarse grids.

Numerical implementation

It is usual to have a theoretical discussion followed by a description of the numerical implementation. Here we will reverse the order because the numerical implementation is so

simple, while the theory is more difficult, at least for those unfamiliar with differential geometry.

Triangle

Figure 3 shows a curvilinear triangle tiled with curvilinear equilateral triangles. The triangle is flat so that it can be seen that the tiles are equilateral, but the same procedure can be used if all nodes are constrained to lie on a given curved surface. The figure was produced by simply setting the coordinates of each interior node equal to the average of the coordinates of the six nodes to which it is connected. Each edge node is slid along its boundary curve until the lengths of the projections of the two blue lines connected to the edge node onto the boundary itself are of equal length.

Algorithm

It is easier to understand the process if we imagine that the lines on the surface are cables under tension. If the tension in each cable is proportional to its length, then static equilibrium means that the coordinates of each node are the average of those to which it is connected. We can also see that if the nodes are constrained to a surface, all we have to do is to allow the nodes to slide over the surface by removing the component of force in the direction of the normal.

In structural mechanics the tension in a member divided by its length is known as the tension coefficient. In German the word Kraftdichte is used, literally, force density. Thus the structural analogy is to use constant tension coefficient cables with nodes that may be constrained to move on a particular surface. Edge nodes are free to slide along the boundary. If the nodes are not constrained to a surface then we shall see that the resulting net forms a minimal surface with a uniform surface tension.

It is possible to make real constant tension coefficient members using coil springs whose coils touch until a certain tension pulls them apart such that the length is proportional to the tension. Such springs were developed by George Carwardine (in Bath) and he used them in the Anglepoise lamp.

The numerical technique finds the equilibrium position by considering the equivalent dynamic problem in which the nodes are moved bit by bit over a large number of cycles. This technique is variously known as dynamic relaxation (invented by Alistair Day), Verlet integration or the semi-implicit Euler, symplectic Euler, semi-explicit Euler, Euler–Cromer or Newton–Størmer–Verlet (NSV) method. The reason for using an iterative technique is that the problem is non-linear unless the nodes are not constrained to move on a surface and the boundaries are straight lines.

Consider a typical internal node, A, whose location is defined by the position vector

$$\mathbf{r}_\mathrm{A} = x_\mathrm{A}\mathbf{i} + y_\mathrm{A}\mathbf{j} + z_\mathrm{A}\mathbf{k}$$

$\mathbf{i}$, $\mathbf{j}$ and $\mathbf{k}$ are unit vectors in the directions of the Cartesian coordinate axes. If it is surrounded by six nodes, B, C, D, E, F, and G, the net force from the six cables is

$$\mathbf{F}_A = \eta(\mathbf{r}_B - \mathbf{r}_A) + \eta(\mathbf{r}_C - \mathbf{r}_A) + \eta(\mathbf{r}_D - \mathbf{r}_A) + \eta(\mathbf{r}_E - \mathbf{r}_A) + \eta(\mathbf{r}_F - \mathbf{r}_A) + \eta(\mathbf{r}_G - \mathbf{r}_A)$$

where η is the constant tension coefficient. If a node is only connected to four nodes then there would only be four contributions to the force.

If the nodes are constrained to move on a surface $\mathbf{F}_A$ is replaced by

$$\mathbf{F}_A - (\mathbf{F}_A \bullet \mathbf{n})\mathbf{n}$$

in which $\mathbf{n}$ is the unit normal to the surface at A and the $\bullet$ denotes the scalar product. This removes the component of $\mathbf{F}_A$ normal to the surface. It is easiest to specify the surface in the form $f(x,y,z) = 0$, because then the unit normal to the surface is

$$\mathbf{n} = \frac{\nabla f}{\sqrt{\nabla f \bullet \nabla f}} = \frac{\frac{\partial f}{\partial x}\mathbf{i} + \frac{\partial f}{\partial y}\mathbf{j} + \frac{\partial f}{\partial z}\mathbf{k}}{\sqrt{\left(\frac{\partial f}{\partial x}\right)^2 + \left(\frac{\partial f}{\partial y}\right)^2 + \left(\frac{\partial f}{\partial z}\right)^2}}.$$

If a node is slightly off the surface it can be put back onto the surface by moving it by $-\left(\frac{f}{\nabla f \bullet \nabla f}\right)\nabla f$.

In a time interval δt the velocity of node A changes from $\mathbf{v}_A$ to

$$(1-\lambda)\mathbf{v}_A + \frac{\mathbf{F}_A}{m}\delta t$$

in which m is the real or fictitious mass of each node and λ is a factor to represent damping. In the same time interval $\mathbf{r}_A$ will change by $\mathbf{v}_A \delta t$.

All the forces on the nodes are calculated in each cycle before updating the velocities and coordinates. The rate of convergence is controlled by the values of λ and $\frac{\eta \delta t^2}{m}$, which are both dimensionless ratios. Typically λ = 0.01 to 0.001 gives the best results and $\frac{\eta \delta t^2}{m}$ is chosen by trial and error, if it is too low the procedure is slow, but if it is too large instability will result.

Icosahedron and sphere

The black lines in figure 4 are the projection of the edges of an icosahedron onto a sphere. The sphere and icosahedron share the same centre and the projection is done using straight lines. If a plane is covered with a grid of straight lines, it can be projected onto the sphere to form geodesics (figure 5), again using straight lines through the centre of the sphere. This is known as gnomonic projection and it is almost certainly what Buckminster Fuller used for his geodesic domes. However in figure 4 the blue lines form equilateral triangles and close examination of the figure shows that the blue lines do have geodesic curvature, that is curvature in the plane of the surface and are therefore not geodesics. It is not possible to have both geodesics and equilateral triangles.

Hexagon and circle, hexagon and sphere

Figures 6 a, b and c show a hexagon relaxed onto a flat circle and onto a sphere. On the sphere the grid is repeated twice, once for the top and once for the bottom, the upper and lower parts of figure 6c. The half squares at the edges of figures 6a and 6b join to form full squares on the sphere.

Circle and square

Figures 7 and 8 attempt the title of this paper, the reconciliation of the circle and the square. There is a clear relationship between figure 8 and figure 2, the main difference being that in figure 2 there is a third set of black lines dividing the quadrilaterals into triangles. The triangles were chosen for the British Museum gridshell primarily for structural reasons. In the numerical work to produce both figures 7b and 8b it was necessary to automatically adjust the diameter of the circle to achieve curvilinear squares rather than curvilinear rectangles. The reason for this is explained in the theoretical discussion.

Frei Otto ‘eye’

Finally, figures 9 and 10 show the Frei Otto ‘eye’. Figure 9 is a physical experiment using washing-up fluid. The trick is to keep the wool loop taut with your fingers while someone else pops the soap film inside the loop. The wool then forms a circle which can be gently pulled up. We will leave discussion of figure 10 for now, except to say that it was formed in the same way as the other figures with the net automatically forming the minimal surface. Soap film surfaces are minimal because the surface tension automatically reduces the surface area to a minimum.

Theoretical discussion

Consider a surface defined by the three equations

$$x = x(u,v)$$
$$y = y(u,v) \text{ or } \mathbf{r} = x(u,v)\mathbf{i} + y(u,v)\mathbf{j} + z(u,v)\mathbf{k}$$
$$z = z(u,v)$$

in which u and v are parameters or surface coordinates and $\mathbf{r}$ is a position vector.

However, we shall not use u and v as parameters, but instead use x^1 and x^2 which are two separate parameters, NOT x to the power one and x squared. The reason for the superscripts is that we can then use the tensor notation. Eisenhart [2] uses parameters u^1 and u^2, whereas Green and Zerna [3] use θ^1 and θ^2. Green and Zerna has the advantage that it covers shell theory, that is the equilibrium of surfaces as well as their geometry. Struik [4] uses u and v are parameters and the following table shows a comparison of the three notations:

Quantity	Struik	Eisenhart	Green and Zerna	This paper
Surface parameters or coordinates	u and v	u^α where α equals 1 or 2	θ^α where α equals 1 or 2	x^i where i equals 1 or 2
Covariant base vectors	$\mathbf{x}_u$ and $\mathbf{x}_v$	-	$\mathbf{a}_\alpha = \mathbf{r}_{,\alpha} = \frac{\partial \mathbf{r}}{\partial x^\alpha}$	$\mathbf{g}_i = \frac{\partial \mathbf{r}}{\partial x^i}$
Contravariant base vectors	-	-	$\mathbf{a}^\alpha$	$\mathbf{g}^i$
Coefficients of the first fundamental form, components of metric tensor	E, F and G	$g_{\alpha\beta}$	$a_{\alpha\beta}$	g_{ij}
Coefficients of the second fundamental form	e, f and g	$d_{\alpha\beta}$	$b_{\alpha\beta}$	b_{ij}
Christoffel symbols	-	$\left\{ \begin{matrix} \lambda \\ \alpha\beta \end{matrix} \right\}$	$\Gamma^\lambda_{\alpha\beta}$	Γ^k_{ij}
Covariant derivative of the components of a vector	-	$v^j{}_{,i}$	$v^j \mid_i$	$\nabla_i v^j$

Quantity	Struik	Eisenhart	Green and Zerna	This paper
Components of membrane stress in a shell	-	-	$n^{\alpha\beta}$	σ^{ij}

Two way net

In a two way net a typical node (i,j), is connected to four neighbours, $(i+1,j)$, $(i,j+1)$, $(i-1,j)$ and $(i,j-1)$. If the tension coefficient is taken as unity, the resulting out of balance force on node (i,j) is the component of

$$\begin{aligned}&\left(\mathbf{r}_{i+1,j}-\mathbf{r}_{i,j}\right)+\left(\mathbf{r}_{i,j+1}-\mathbf{r}_{i,j}\right)+\left(\mathbf{r}_{i-1,j}-\mathbf{r}_{i,j}\right)+\left(\mathbf{r}_{i,j-1}-\mathbf{r}_{i,j}\right)\\&=\left(\mathbf{r}_{i+1,j}-2\mathbf{r}_{i,j}+\mathbf{r}_{i-1,j}\right)+\left(\mathbf{r}_{i,j+1}-2\mathbf{r}_{i,j}+\mathbf{r}_{i,j-1}\right)\end{aligned}$$

in the local tangent plane to the surface. The equivalent continuum quantity is the component of

$$\frac{\partial}{\partial x^1}\left(\frac{\partial \mathbf{r}}{\partial x^1}\right)+\frac{\partial}{\partial x^2}\left(\frac{\partial \mathbf{r}}{\partial x^2}\right)=\frac{\partial^2\mathbf{r}}{\left(\partial x^1\right)^2}+\frac{\partial^2\mathbf{r}}{\left(\partial x^2\right)^2}=\frac{\partial \mathbf{g}_1}{\partial x^1}+\frac{\partial \mathbf{g}_2}{\partial x^2}$$

in the local tangent plane. Thus for equilibrium,

$$\begin{aligned}\left(\frac{\partial \mathbf{g}_1}{\partial x^1}+\frac{\partial \mathbf{g}_2}{\partial x^2}\right)\bullet\mathbf{g}_1=0\\\left(\frac{\partial \mathbf{g}_1}{\partial x^1}+\frac{\partial \mathbf{g}_2}{\partial x^2}\right)\bullet\mathbf{g}_2=0\end{aligned}.$$

The components of the metric tensor, $g_{ij}=\mathbf{g}_i\bullet\mathbf{g}_j$, and therefore

$$\begin{aligned}\frac{\partial g_{jk}}{\partial x^i}&=\frac{\partial \mathbf{g}_j}{\partial x^i}\bullet\mathbf{g}_k+\mathbf{g}_j\bullet\frac{\partial \mathbf{g}_k}{\partial x^i}\\\frac{\partial g_{ki}}{\partial x^j}&=\frac{\partial \mathbf{g}_k}{\partial x^j}\bullet\mathbf{g}_i+\mathbf{g}_k\bullet\frac{\partial \mathbf{g}_i}{\partial x^j}\\\frac{\partial g_{ij}}{\partial x^k}&=\frac{\partial \mathbf{g}_i}{\partial x^k}\bullet\mathbf{g}_j+\mathbf{g}_i\bullet\frac{\partial \mathbf{g}_j}{\partial x^k}\\\frac{\partial \mathbf{g}_i}{\partial x^j}\bullet\mathbf{g}_k&=\frac{1}{2}\left(\frac{\partial g_{jk}}{\partial x^i}+\frac{\partial g_{ki}}{\partial x^j}-\frac{\partial g_{ij}}{\partial x^k}\right)\end{aligned}$$

since $\frac{\partial \mathbf{g}_i}{\partial x^j}=\frac{\partial^2\mathbf{r}}{\partial x^i\partial x^j}=\frac{\partial \mathbf{g}_j}{\partial x^i}$.

Thus the equilibrium equations become

$$\frac{1}{2}\left(\frac{\partial g_{1k}}{\partial x^1}+\frac{\partial g_{k1}}{\partial x^1}-\frac{\partial g_{11}}{\partial x^k}\right)+\frac{1}{2}\left(\frac{\partial g_{2k}}{\partial x^2}+\frac{\partial g_{k2}}{\partial x^2}-\frac{\partial g_{22}}{\partial x^k}\right)=0$$

for $k=1$ and $k=2$. The metric tensor is symmetric ($g_{ij}=g_{ji}$) and so

$$\frac{\partial g_{k1}}{\partial x^1}-\frac{1}{2}\frac{\partial g_{11}}{\partial x^k}+\frac{\partial g_{k2}}{\partial x^2}-\frac{1}{2}\frac{\partial g_{22}}{\partial x^k}=0$$

or

$$\begin{aligned}\frac{1}{2}\frac{\partial}{\partial x^1}\left(g_{11}-g_{22}\right)+\frac{\partial g_{12}}{\partial x^2}&=0\\ -\frac{1}{2}\frac{\partial}{\partial x^2}\left(g_{11}-g_{22}\right)+\frac{\partial g_{12}}{\partial x^1}&=0\end{aligned}.$$

These are the Cauchy–Riemann equations and produce

$$\begin{aligned}\frac{\partial^2}{\left(\partial x\right)}\left(g_{11}-g_{22}\right)+\frac{\partial^2}{\left(\partial x\right)}\left(g_{11}-g_{22}\right)&=0\\ \frac{\partial^2 g}{\left(\partial x\right)}+\frac{\partial^2 g}{\left(\partial x\right)}&=0\end{aligned}.$$

Thus both $\left(g_{11}-g_{22}\right)$ and g_{12} satisfy Laplace's equation. Note that here we have just partial derivatives, NOT covariant derivatives which one would normally associate with differential equations on a surface.

Examination of figures 7a and 7b shows that the sliding boundary condition means that the cables are orthogonal on all boundaries, except at the singular points corresponding to the corners of the inner square. Adjustment of the circle radius removes this problem to produce $g_{12}=0$ on all boundaries, and therefore Laplace's equation tells us that $g_{12}=0$ everywhere. Thus $\frac{\partial}{\partial x^1}\left(g_{11}-g_{22}\right)=0$ and $\frac{\partial}{\partial x^2}\left(g_{11}-g_{22}\right)=0$ so that $g_{11}-g_{22}=\text{constant}$ everywhere. Thus we must have curvilinear rectangles, all with the same difference in the square of the side lengths. In the case of figure 7b symmetry tells us that the rectangles must be squares – provided that we have the correct circle radius to ensure $g_{12}=0$.

The sphere in figure 6c has no boundaries, although it does have eight poles, whereas the sphere in figure 4 has twelve poles. In figure 8b the boundary conditions are mixed. On the circle and towards the middle of each side $g_{11}-g_{22}=0$, whereas towards the ends of each side $g_{12}=0$. Again it was necessary to adjust the circle diameter to achieve curvilinear squares.

Generalisation

A net with curvilinear squares and constant tension coefficients corresponds to a uniform surface tension equal to the tension coefficient. A uniform surface tension in a general coordinate system corresponds to the membrane stress tensor (see Green and Zerna [3]) being proportional to the metric tensor, or in components,

$$\sigma^{ij} = \eta g^{ij}$$

in which η is the surface tension.

Let us imagine an initial or reference configuration in which the contravariant components of the metric tensor are G^{ij}. If we want have a conformal mapping from this configuration to a new configuration, then in the new configuration $g^{ij} = \frac{\sqrt{G}}{\sqrt{g}} G^{ij}$ in which $G = G_{11}G_{22} - G_{12}^2$ and $g = g_{11}g_{22} - g_{12}^2$. A conformal map is one which preserves angles and ratios of lengths.

Now if we set $\sigma^{ij} = \frac{\sqrt{G}}{\sqrt{g}} G^{ij}$, the equilibrium equations in the local tangent plane of the new surface are

$$0 = \nabla_i \sigma^{im} = \frac{\partial}{\partial x^i}\left(\frac{\sqrt{G}}{\sqrt{g}} G^{im} \right) + \frac{\sqrt{G}}{\sqrt{g}} G^{jm} \Gamma^i_{ij} + \frac{\sqrt{G}}{\sqrt{g}} G^{ij} \Gamma^m_{ij}$$

in which ∇_i is the covariant derivative and $\Gamma^m_{ij} = g^{mk} \frac{1}{2}\left(\frac{\partial g_{jk}}{\partial x^i} + \frac{\partial g_{ki}}{\partial x^j} - \frac{\partial g_{ij}}{\partial x^k} \right)$ are the Christoffel symbols. We can use the fact that

$$\Gamma^i_{ij} = g^{ik} \frac{1}{2}\left(\frac{\partial g_{jk}}{\partial x^i} + \frac{\partial g_{ki}}{\partial x^j} - \frac{\partial g_{ij}}{\partial x^k} \right) = g^{ik} \frac{1}{2} \frac{\partial g_{ki}}{\partial x^j} = \frac{1}{\sqrt{g}} \frac{\partial \sqrt{g}}{\partial x^j}$$

to write

$$\frac{\partial}{\partial x^i}\left(\sqrt{G} G^{im} \right) + \frac{\sqrt{G} G^{ij} g^{mk}}{2} \left(\frac{\partial g_{jk}}{\partial x^i} + \frac{\partial g_{ki}}{\partial x^j} - \frac{\partial g_{ij}}{\partial x^k} \right) = 0 .$$

Finally we can use the Levi-Civita tensor or permutation tensor to write

$$\frac{\partial}{\partial x^i}\left(\sqrt{G} G^{im} \right) + \frac{\sqrt{G} G^{ij} \varepsilon^{mp} \varepsilon^{kq} g_{pq}}{2} \left(2 \frac{\partial g_{jk}}{\partial x^i} - \frac{\partial g_{ij}}{\partial x^k} \right) = 0$$

in which $\varepsilon^{12} = -\varepsilon^{21} = \frac{1}{\sqrt{g}}$, $\varepsilon^{11} = 0$ and $\varepsilon^{22} = 0$.

If we return to the special case of the curvilinear squares, then $G^{11}=1$, $G^{22}=1$, $G^{12}=0$ and $G=1$, so that

$$2\frac{\partial g_{1k}}{\partial x^1}-\frac{\partial g_{11}}{\partial x^k}+2\frac{\partial g_{2k}}{\partial x^2}-\frac{\partial g_{22}}{\partial x^k}=0$$

which produces

$$\frac{1}{2}\frac{\partial}{\partial x^1}(g_{11}-g_{22})+\frac{\partial g_{12}}{\partial x^2}=0$$
$$-\frac{1}{2}\frac{\partial}{\partial x^2}(g_{11}-g_{22})+\frac{\partial g_{12}}{\partial x^1}=0$$

as above.

Equilateral triangular nets

If we have a uniform equilateral triangular net in the initial configuration, then $G^{11}=1$, $G^{22}=1$, $G^{12}=-\frac{1}{\cos 60^\circ}=-2$ and $G=\frac{1}{1-\cos^2 60^\circ}=\frac{4}{3}$ so that

$$2\frac{\partial g_{1k}}{\partial x^1}-\frac{\partial g_{11}}{\partial x^k}+2\frac{\partial g_{2k}}{\partial x^2}-\frac{\partial g_{22}}{\partial x^k}-2\left(2\frac{\partial g_{2k}}{\partial x^1}-\frac{\partial g_{12}}{\partial x^k}+2\frac{\partial g_{1k}}{\partial x^2}-\frac{\partial g_{21}}{\partial x^k}\right)=0$$

or

$$\frac{\partial}{\partial x^1}(g_{11}-g_{22})=4\frac{\partial g_{11}}{\partial x^2}-2\frac{\partial g_{12}}{\partial x^2}$$
$$-\frac{\partial}{\partial x^2}(g_{11}-g_{22})=4\frac{\partial g_{22}}{\partial x^1}-2\frac{\partial g_{12}}{\partial x^1}$$

These are satisfied by $g_{11}=g_{22}=2g_{12}$ which is the requirement for a curvilinear equilateral triangle net.

Minimal surfaces

A minimal surface is a surface of minimum surface area which can be physically modelled by a soap film. Minimal surfaces have many interesting properties, amongst whish is the fact that the principal curvature trajectories form curvilinear squares on the surface. On a minimal surface the asymptotic directions (which are the directions of zero normal curvature) are at 45º to the principal curvature directions and therefore their trajectories also form curvilinear squares on the surface.

If a soap film has a boundary which is a thread under tension, then equilibrium of the thread dictates that the curvature of the thread must be constant and lie in the local tangent plane to the soap film surface. This means that the boundary must be an asymptotic trajectory. And these facts were used to produce the minimal surface in figure 10. The nodes are free to

move in the direction normal to the surface, automatically producing a minimal surface. The main problem is the adjustment of the thread length and the cutting pattern in order to produce curvilinear squares. Included in this adjustment is the fact that the maximum slope along the straight edges must occur at a point where the curvilinear squares are theoretically infinitely large.

Conclusions

The technique provides a relatively simple method of tiling a surface with curvilinear tiles of constant shape, but varying size. In the case of a triangular region equilateral triangles can always be used, but for other shapes care must be taken with the boundary conditions to ensure that the tiles are of the same shape. For minimal surfaces, the technique can both find the shape and produce a principal curvature or, alternatively, an asymptotic direction net.

In this paper we have used the Laplace's equation, or the harmonic equation, associated with the operator ∇^2. This means that we have one boundary condition. The biharmonic equation, associated with ∇^4, allows two boundary conditions, for example the position and slope of a bent elastic plate. The flow of fluids in two dimensions can be modelled using an analogy of a bent plate in which mean curvature of the plate is equal to the fluid vorticity. Figure 11 was produced this way using techniques not that dissimilar to those employed in this paper. The black streamlines are the contours of height of the plate and the blue streak shows the starting of vortex shedding. The reason for including this figure is to demonstrate the complexity of patterns that develop in nature, again effectively from the interaction of rectangular and circular geometries.

References

1. Chris J K Williams, C.J.K. 'The definition of curved geometry for widespan structures', 41-49, *Widespan roof structures*, Barnes, M. and Dickson, M. eds. Thomas Telford, London, 2000, ISBN 0 7277 2877 6.

2. Luther Pfahler Eisenhart, *An Introduction to Differential Geometry with Use of the Tensor Calculus*, Princeton University Press, 1940.

3. A E Green and W Zerna, *Theoretical Elasticity*, 2nd Edition, Oxford University Press, 1968.

4. Dirk J. Struik, *Lectures on Classical Differential Geometry*, 2nd Edition, Dover Publications, 1988.

Figures

Figure 1 *The British Museum Great Court Roof by Foster + Partners, Buro Happold and Waagner-Biro*

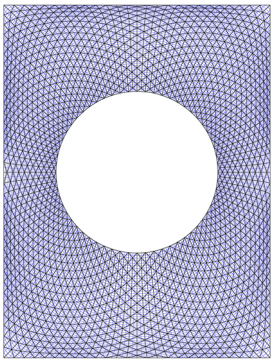

Figure 2 *Great Court Roof structural and 'mathematical' grids*

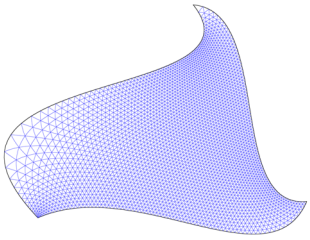

Figure 3 *Curvilinear triangle tiled with curvilinear equilateral triangles*

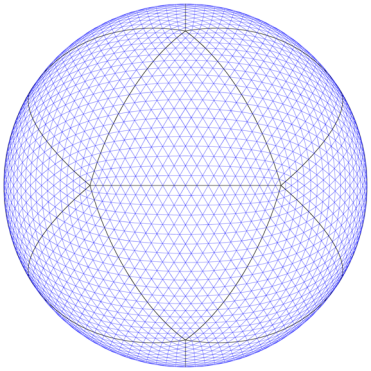

Figure 4 *Icosahedron projected on sphere (black lines) with equilateral triangle infill (blue lines)*

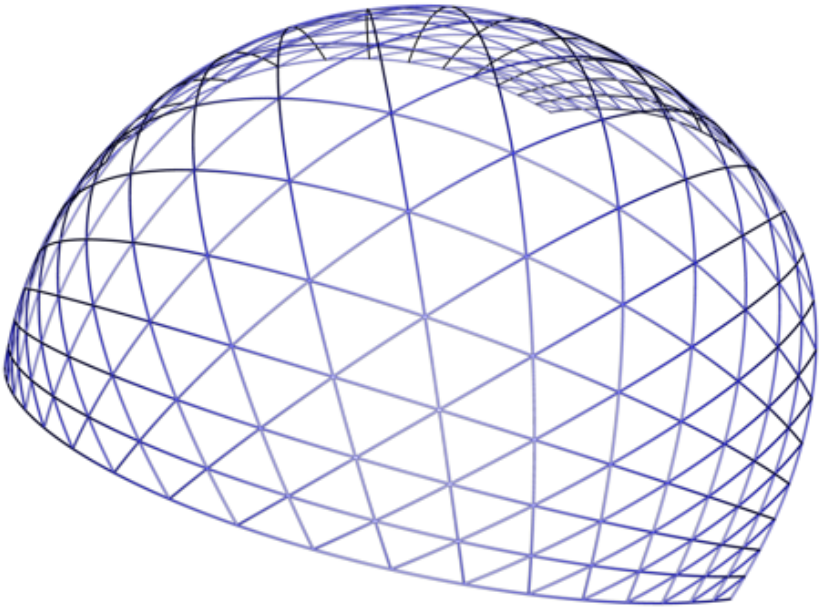

Figure 5 *Three – way geodesics on sphere by gnomonic projection*

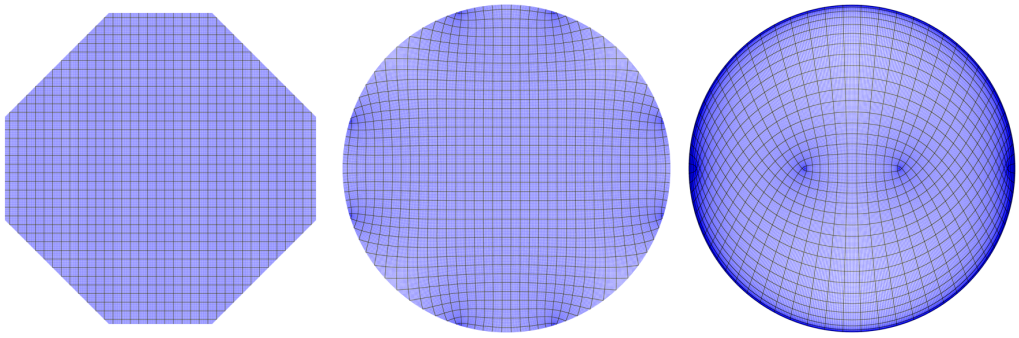

Figure 6 *Hexagonal grid*: *(a) cutting pattern, (b) relaxed into flat circle and (c) relaxed onto sphere*

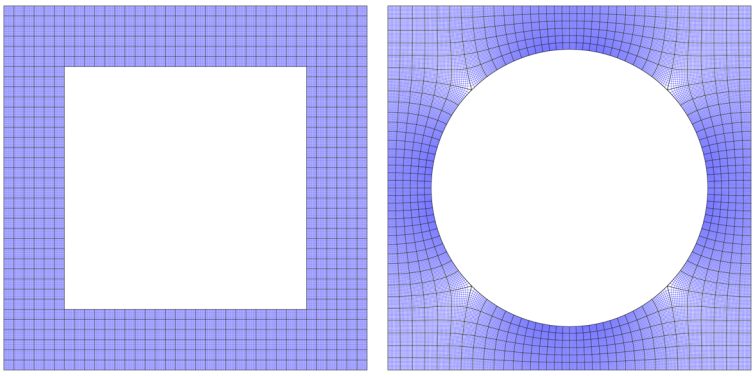

Figure 7 *Square grid with cut out*: *(a) cutting pattern and (b) relaxed with central circle*

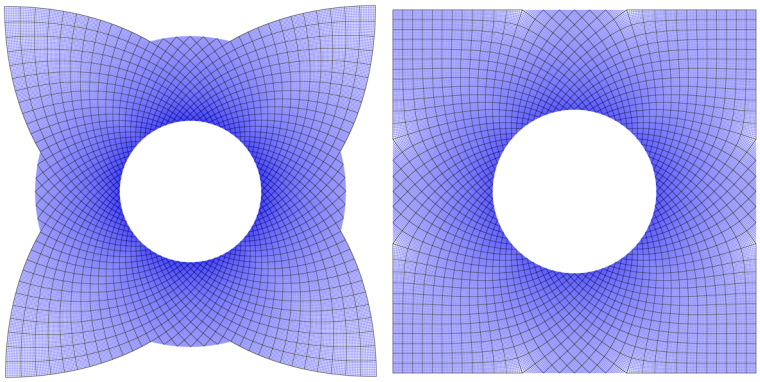

Figure 8 *Spiral grid*: *(a) cutting pattern and (b) relaxed with outer square*

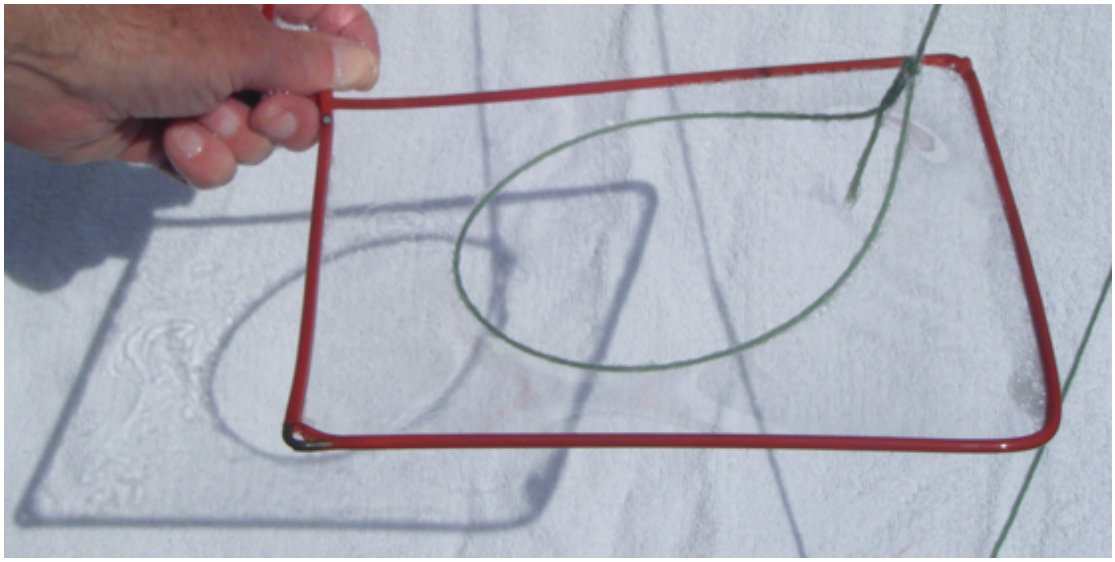

Figure 9 *Frei Otto 'eye' soap film experiment*

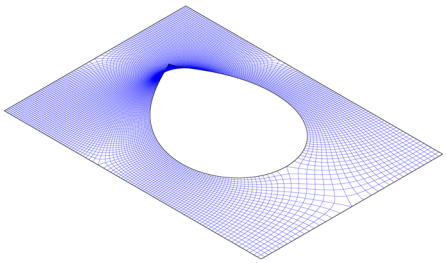

Figure 10 *Frei Otto 'eye' asymptotic lines on the surface forming curvilinear squares*

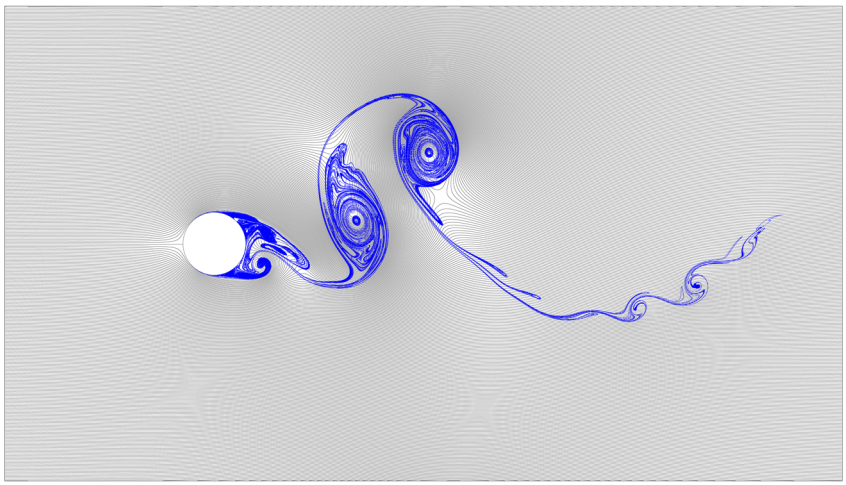

Figure 11